JOURNAL OF SPACECRAFT AND ROCKETS
Vol. 40, No. 5, September–October 2003

Flight-Dynamics Instability Induced by Heat-Shield Ablation Lag Phenomenon

T. C. Lin,* L. K. Sproul,* and M. Olmos*
TRW Systems, San Bernardino, California 92402
and
N. A. Thyson†
Textron Systems, Wilmington, Massachusetts 01864

Flight-dynamics instabilities resulting from the ablation-lag phenomenon have been investigated. Ablation lag occurs on spin-stabilized missiles or reentry vehicles that use ablative materials for thermal protection. The present approach includes the coupling and combined effects of reentry vehicle surface recession, heat conduction into the vehicle skin, reentry vehicle spin rate, and angle of attack. Thyson's analysis on the magnitude of ablation lag is used in the present analysis. The present model predicts the advent of reentry-vehicle flight instability during reentry and the eventual self-curing of the divergence. The thermal performance of several heat-shield materials and the propensity of the materials to induce flight instability are briefly assessed. Numerical examples are given to illustrate the ablation-lag phenomenon.

Nomenclature

A	=	amplitude of ablation oscillation
B'	=	nondimensional ablation parameter [see Eq. (7)]
C_1, C'	=	constant defined in Eq. (9)
$C_{m_q} + C_{m_{\dot\alpha}}$	=	aerodynamic pitch damping
C_N	=	normal-force coefficient
C_n	=	out-of-plane moment coefficient
C_p	=	specific heat
C_Y	=	yaw-force coefficient
H_v	=	total enthalpy of the gas at the wall
H_{0w}	=	heat-shield surface enthalpy
I_x, I_y	=	reentry-vehicle moments of inertia
$\hat{i}_y, \hat{i}_N$	=	unit vectors in wind-fixed coordinates
L	=	vehicle length
L_{ref}	=	reference length
L_V	=	heat of vaporization or sublimation
M_{air}	=	molecular weight of air
M_{inj}	=	molecular weight of injected gases
$\dot{m}$	=	surface ablation flux
p	=	reentry-vehicle spin rate
Q^*	=	heat of ablation for ablative heat-shield material
$\dot{q}$	=	wall heat flux
R	=	parameter used in defining angle-of-attack history in BK-9 flight data, deg
S	=	parameter used in defining angle-of-attack history in BK-9 flight data, deg
$\dot{s}$	=	heat-shield surface ablation rate
$\dot{s}_0$	=	steady-state heat-shield surface ablation rate
T	=	heat-shield material local temperature
t	=	time
V	=	missile/reentry-vehicle velocity
y	=	distance normal to ablating surface
α	=	angle of attack
Δ	=	viscous displacement thickness
ζ	=	nondimensional aerodynamic damping
θ_c	=	half-coning angle
κ	=	heat-shield thermal conductivity
Λ	=	$\omega\lambda/\dot{s}_0^2$
λ	=	$\kappa/(\rho C_p)$, thermal diffusivity
ν	=	$\mu/\rho(\mu =$ gas viscosity)
ρ	=	heat-shield material density
ρ_g	=	pyrolysis gas density
ρ_w	=	gas density at surface
σ	=	Stefan–Boltzmann constant or the ratio of instantaneous ablation rate to the steady-state ablation rate [Eq. (4)]
ϕL	=	ablation phase lag (phase difference between the peak heating and peak ablation rate)
$\dot{\psi}$	=	precession rate
ω	=	missile/reentry-vehicle spin/oscillation rate
ϖ	=	missile/reentry-vehicle undamped natural pitch frequency

Received 28 May 2002; revision received 3 January 2003; accepted for publication 6 January 2003.

*Member of Technical Staff, Missile Defense Division. Member AIAA.
†Director, Missile Systems. Member AIAA.

Introduction

WHEN a missile or reentry vehicle (RV) is at an angle of attack, the peak heating rates occur at the windward plane. Because the spin-stabilized missile/RV is in precession/spinning motion and the heat-shield ablation rate does not instantaneously react to the transient heating impulse, a lag occurs in heat-shield recession with the peak heating. This is referred to as "ablation lag."

This thermodynamic time lag is caused, in part, by the heat-shield material's finite thermal diffusivity. In most instances, the lag does not cause a flight-dynamics instability. However, angle-of-attack divergence and range dispersion do occur on certain missiles, RVs, or decoys using special heat shields. Some scientists have attributed the flight anomalies observed on those flights to ablation lag.

Waterfall[1] first proposed the idea of ablation lag to explain the observed anomalies that occurred on a British Black Knight-9 flight (BK-9). He found that a time lag of 0.04 s (or a phase lag of 55 deg for a spin rate of 24 rad/s) is needed to give a good fit to BK-9 flight data.

Morrison and Fiscina[2] performed wind-tunnel experiments to measure the ablation-lag moments on a spinning, ablating camphor model at angle of attack. Their data indicate the existence of an out-of-plane moment, which would increase the aerodynamic damping and alter the pitching and yawing frequencies.

Martellucci and Neff[3] proposed that the asymmetric boundary-layer transition on a slender reentry vehicle can cause flight instability and transient angle-of-attack divergence. The combined effects of surface mass transfer and asymmetric transition have a strong

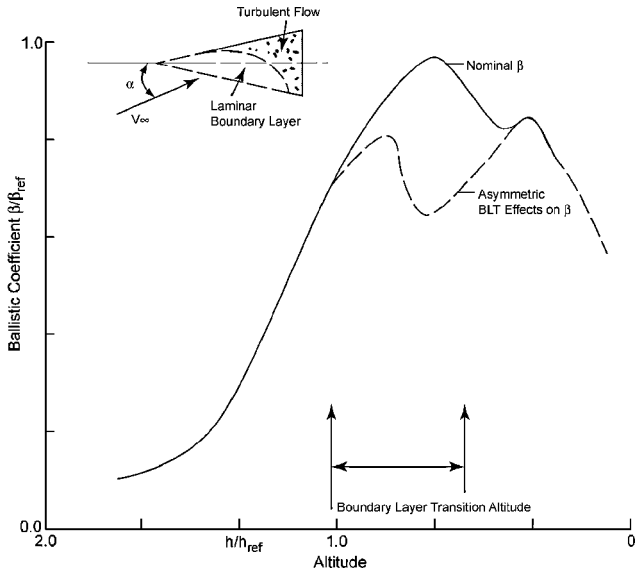

Fig. 1 Ballistic coefficient variation with altitude with asymmetric boundary-layer transition effects.[3]

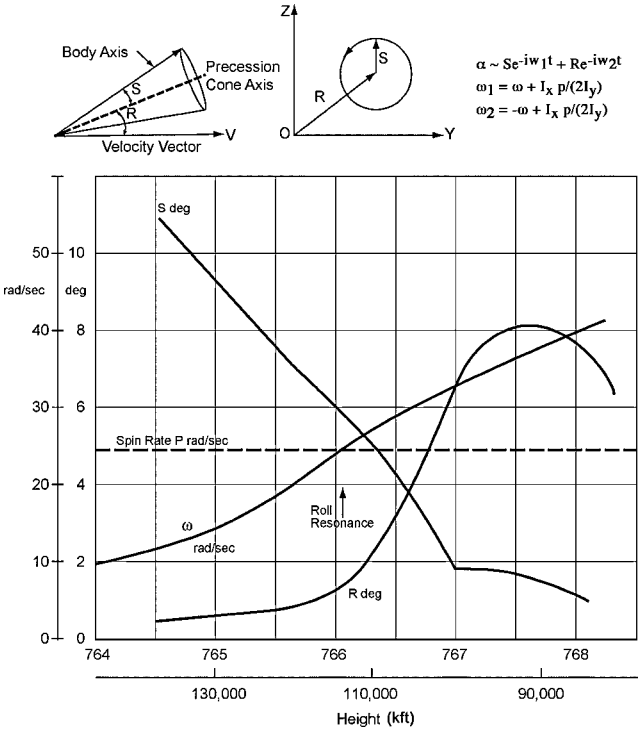

Fig. 2 Black Knight-9 flight data.[1]

influence on the motion of a reentry vehicle. Figure 1 depicts the RV ballistic coefficient history β, which indicates a large decrease in β during boundary-layer transition. Martellucci and Neff's wind-tunnel test results indicated a decrease in RV static stability characteristics during boundary-layer transition, which would, in turn, induce a temporal angle-of-attack divergence.

Figure 2 depicts BK-9 flight dynamics in the altitude range from 140 to 70 kft. Reference 1 presents the flight data using epicyclic motion analysis, that is, the angle of attack is written as the vector sum of two arms S and R, as $\alpha = Se^{(-i\omega_1 t)} + Re^{(-i\omega_2 t)}$. On BK-9 the angle of attack α diverged in the altitude range $130 < h < 70$ kft. Below 130 kft, α or R started to increase; eventually, R began to converge below 80 kft. Note that angle-of-attack divergence began to occur at a higher altitude than the roll resonance altitude. The roll resonance occurred at 113 kft (Fig. 2), and no angle-of-attack divergence resulting from body mass or configuration asymmetry

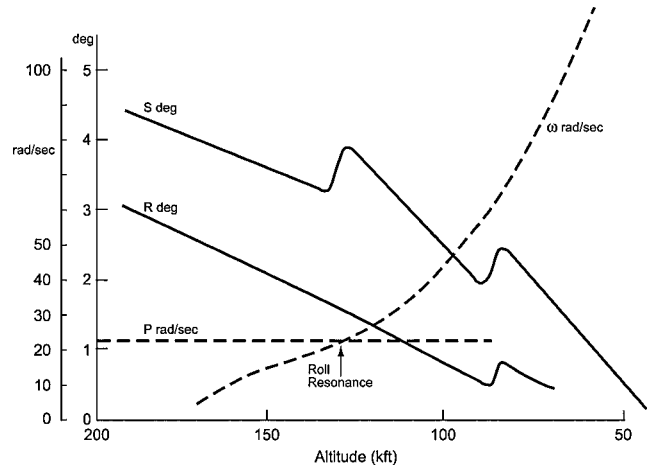

Fig. 3 Flight data on Black Knight-18.[1]

was detected on BK-9. This is based on observation of the history of S (Ref. 1).

For the purpose of thermal protection during ascent flight, the BK-9 vehicle was given a thin layer of coating at its outer heat shield. The coating material was Araldite. However, the coating material started to ablate significantly during reentry below 150 kft altitude, when RV instability began.[1]

To explain this flight anomaly, a similar flight test was conducted with an almost identical vehicle configuration and thermal protection system. One difference was that the RV (Black Knight 18, or BK-18) had no overlay material (Araldite). As Fig. 3 shows, BK-18 exhibited completely different flight behavior (i.e., no large angle-of-attack divergence). It experienced a small angle-of-attack increase at roll resonance altitude and a second angle-of-attack increase at or near the boundary-layer transition altitude. Evidently, BK-18 had more mass and configuration asymmetries than BK-9. This is reflected in the α, or S, divergence at roll resonance altitude.

Some researchers attempted to explain BK-9's flight anomaly (the angle-of-attack divergence) at high altitude by postulating the advent of a large, positive dynamic stability damping, $C_{m_q} + C_{m_{\dot\alpha}} \gg 1$. Some success was noted with this postulation; however, no physical mechanism could be visualized to produce this large, unstable stability derivative ($C_{m_q} + C_{m_{\dot\alpha}} \gg 1$).

The purpose of the present paper is to assess and quantify this lag phenomena and develop analytical models inferred from first principles to estimate the magnitude of the phase lag as well as the associated magnitude of the induced out-of-plane moments. In particular, the types of heat shields, levels of ablation rate, and spin rates that would induce flight instability are identified and investigated.

We will first present an approximate solution for the ablation lag for general noncharring heat-shield materials. Then the induced out-of-plane moment (or Magnus moment) will be derived based on the asymmetric viscous displacement effects caused by the heat-shield ablation-lag phenomenon. Finally, flight simulations will be made using the derived out-of-plane moments to assess the conditions under which the flight instability would occur.

Ablation Lag/Thermal Conduction[4]

The one-dimensional, transient heat-conduction equation for a noncharring ablator is written as

$$\rho C p \frac{\partial T}{\partial t} = \frac{\partial}{\partial y}\left(\kappa \frac{\partial T}{\partial y}\right) + \dot{s}\rho C p \frac{\partial T}{\partial y} \tag{1}$$

The origin of the coordinate $y = 0$ is attached to the ablated surface. The boundary conditions for Eq. (1) are the surface energy balance at $y = 0$ and the conditions as $y \to \infty$, that is,

$$\dot{q} - \sigma T_w^4 = -\kappa T_y + \dot{m} H_v \qquad \text{at} \qquad y = 0$$

$$T = T_i \qquad \text{as} \qquad y \to \infty \tag{2}$$

Heat-shield ablation can be estimated by using a thermal-chemical equilibrium model (e.g., the use of B' tables), the Q^* model (heat of ablation model), or the Munson–Spindler relation. The Munson–Spindler relation (with appropriate material-dependent constants, C_2, n, C'') can be written as

$$\dot{s} = C_2 T_w^{(-n)} \exp(-C''/T_w) \tag{3}$$

With these equations one can proceed to calculate the missile/RV in-depth temperature profiles and the surface ablation history. In this study the heat-shield materials considered are Teflon®, epoxy, and carbon. Figure 4 illustrates a representative result for epoxy on a 6.3-deg cone spinning at 10 Hz and at 2-deg angle of attack. The oscillating heat transfer input to the surface caused by the angle of attack and the corresponding surface ablation flux $\dot{m}$ are also given in the figure. A phase lag of 40 deg between the peak heating and peak recession rate is noted from the transient heat-conduction computations. The amplitude of the ablation rate oscillation $\dot{m}_{\max}/\dot{m}_{\min}$ is found to be smaller than the amplitude of heat-transfer rate oscillation $\dot{q}_{\max}/\dot{q}_{\min}$. Figure 5 depicts the phase lag angle for Teflon and epoxy at different spin rates.

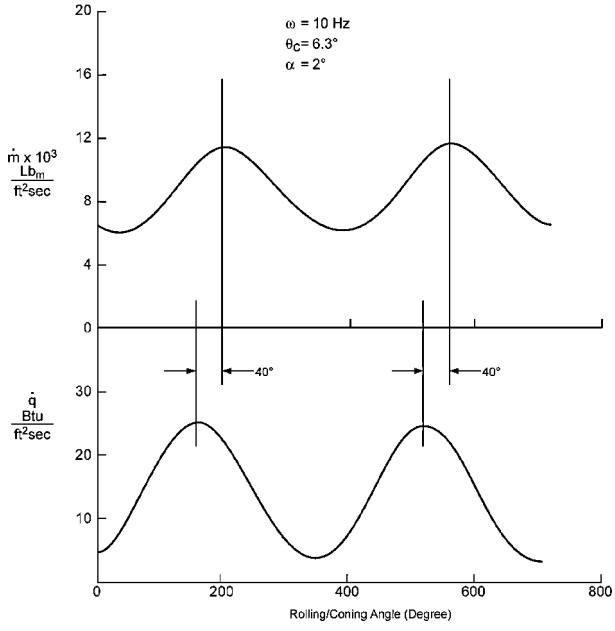

Fig. 4 Ablation lag for epoxy heat shield.

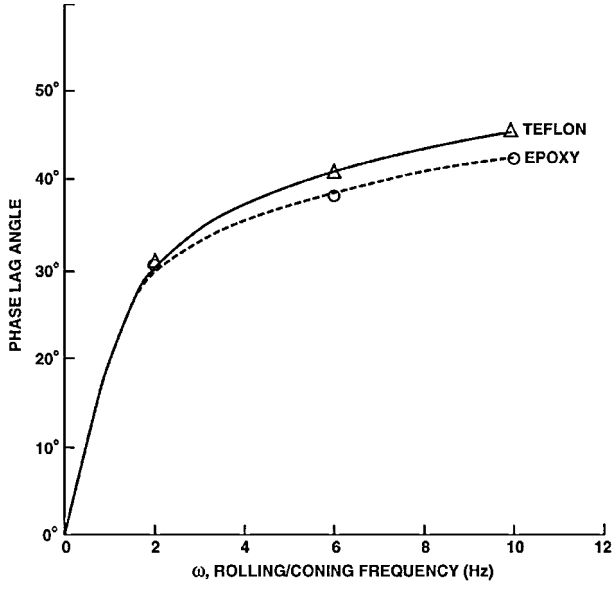

Fig. 5 Phase lag for two heat-shield materials.

Thyson performed a perturbation analysis[4] and was able to derive a closed-form solution in asymptotic series form for the ablation-lag problem from the basic one-dimensional transient heat-conduction equation. His formulation is provided next with a brief discussion.

In nondimensional form the unsteady heat-conduction equation (1) becomes

$$\Lambda\theta_\tau - \sigma\theta_\eta = \theta_{\eta\eta} \tag{4a}$$

and the boundary conditions under Thyson's analysis[4] become

$$\eta = \frac{y\dot{s}_0}{\lambda = 0}, \qquad \theta = \frac{T - T_\infty}{T_{w0} - T_\infty} = \theta_w$$

$$\eta \to \infty, \qquad \theta = 0$$

The quantities σ and θ are taken to perform small oscillations about their steady mean, zero-angle-of-attack values, and can be written as

$$\sigma = \dot{s}/\dot{s}_0 = 1 + \sigma_1 \alpha e^{(i\tau)} \tag{4b}$$

$$\sigma_1 = Ae^{(i\phi_L)}$$

The amplitude A and the phase lag ϕ_L are expressed as a function of $\Lambda = \omega\lambda/\dot{s}_0^2$ (where $\lambda = \kappa/\rho C_p$) and heat-shield material thermal properties. Results for A and ϕ_L from Ref. 4 are depicted in Fig. 6. Thyson's results indicate that the maximum phase lag is 45 deg. Also, the amplitude of the oscillation approaches zero at very high frequency (or $\Lambda \gg 1$). Another interesting result is the prediction of the possible occurrence of "ablation lead" (see Fig. 5, for $\Lambda < 5$). Numerical results given in Figs. 3 and 4 agree reasonably well with the closed-form solutions of Ref. 4.

Figure 6 indicates that there are two important limits. At high altitude when the ablation rate is small because of the low heating level, $\dot{s} \ll 1$ or $\Lambda \gg 1$, the phase lag angle is large and approaches 45 deg. But the amplitude of oscillation is small. Consequently, the combined effects of ablation phase lag and surface ablation on the wall-pressure perturbation induced by viscous displacement effects and aerodynamics can be small.

The other limit is at low altitude, where the heat-transfer rate is high, then $\Lambda \to 0$. Now the phase lag angle becomes small. This situation reduces the transient heat-conduction problem to the steady state [see Eq. (6a)]. The RV heat-shield will react almost instantaneously to the sinusoidal heat-transfer input caused by angle of attack on a spinning reentry vehicle (i.e., no ablation-lag effects). Therefore, the heat-shield ablation will not cause asymmetric aerodynamics or out-of-plane moment. These two limits are important in explaining the flight behavior on BK-9.

One important result from Ref. 4 is the delineation of the various nondimensional timescales.

Ratio of characteristic convection time to characteristic motion time = aerodynamic timescale:

$$[\tau_{\text{inviscid}}] = \omega L/V$$

Ratio of characteristic thermal diffusion time to characteristic motion time = solid thermal diffusion timescale:

$$[\tau_{\text{thermal}}] = \frac{\omega\kappa}{\rho C_p \dot{s}_0^2}$$

In most reentry problems $\tau_{\text{inviscid}} \ll 1$, while $\tau_{\text{thermal}} = \mathcal{O}(1)$ or $\gg 1$. The important observation from the unsteady ablation study is that the aerodynamic time scale (or $\tau_{\text{inviscid}} \ll 1$) is small compared to the solid thermodynamic timescale. Therefore the use of steady aerodynamics and convective heating in conjunction with unsteady surface ablation is justified. Alterations in surface ablation produced by unsteady heating or shear will dominate over changes caused by unsteady aerodynamics.

The formulation just given is for a noncharring ablator. For heat shields with internal pyrolysis/outgassing ($\dot{m}_g = \rho_g v_g$), in addition to wall recession ($\dot{m}_c = \rho_w \dot{s}$) the analysis is more complicated and does not lend itself to a closed-form solution. Therefore, a numerical solution method is required. At high altitudes, where the heat-transfer rates are low, only outgassing occurs ($\rho_g v_g > 0$), and the

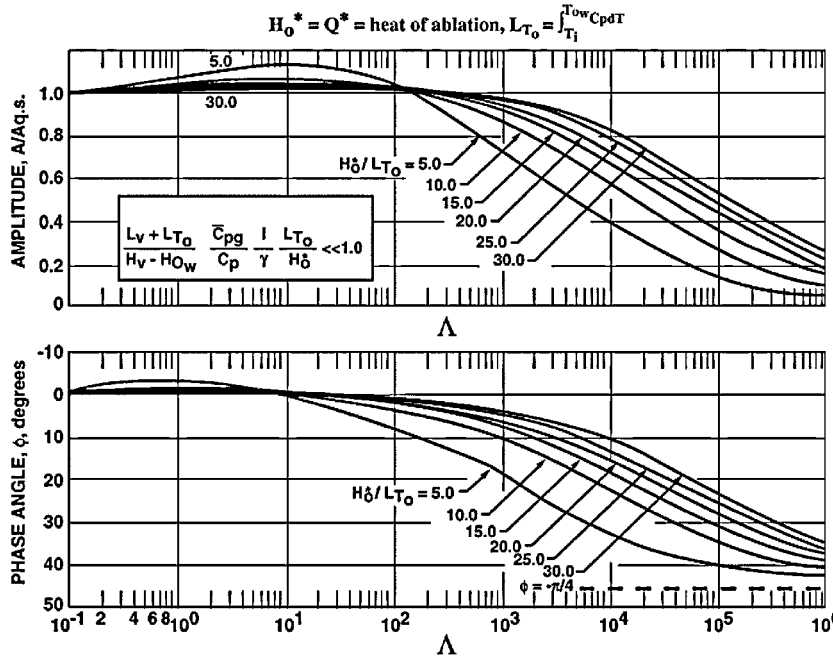

Fig. 6 Oscillatory ablation response (phase angle and amplitude) (from Thyson[4]).

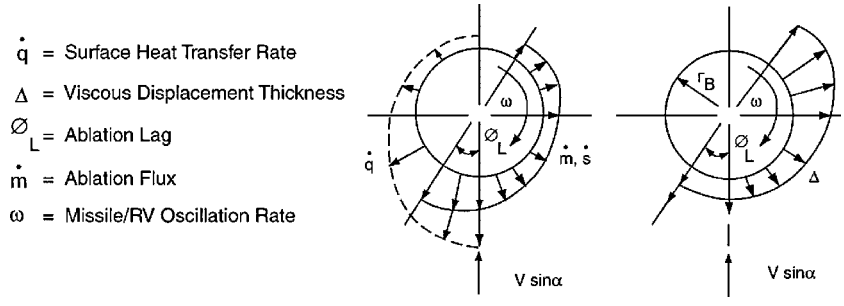

Fig. 7 Ablation-induced displacement thickness on a spinning body.

analysis[5] indicates that a phase lead might result. At lower altitudes, where the heat-transfer rates are higher and outgassing and surface recession occur, both ablation lag and lead are possible.[5]

Aerodynamics (Out-of-Plane Moment)

Two physical mechanisms have been found to be responsible for the occurrence of missile/RV flight-dynamics instability. They are the so-called "Magnus phenomenon" (or the advent of an out-of-plane moment) and the roll resonance phenomenon. Originally, Magnus effects were postulated to explain the flight instability observed on artillery shells spinning at very high rates. Herein, we will develop an aerodynamic model to describe the advent of an out-of-plane moment caused by heat-shield ablation coupled with missile/RV spinning motion. In our case the missile/RV spin rates are much lower than those of artillery shells.

When the heat shield starts to ablate under hypersonic flow heating, it creates an equivalent body shape that causes an induced pressure caused by viscous displacement effects. When there is an ablation lag caused by the spinning, pitching, and precession motion of the missile/RV, the resulting viscous-induced pressure will be asymmetric to the wind plane (Fig. 7). Consequently, it results in a net yaw force and a yaw moment. The asymmetric body shape can be constructed as

$$r_{\text{EFFECTIVE}} = r_B + \Delta \tag{5}$$

where r_B represents the body local radius. Δ can be defined as

$$\Delta = \int_0^\infty \left(1 - \frac{\rho u}{\rho_e u_e}\right) \mathrm{d}y + \int_0^x \frac{\dot{m}}{(\rho_e u_e)} \mathrm{d}x \tag{6}$$

Because of the ablation lag, the effective body shape will not be symmetric to the wind plane. Figure 7 illustrates this phenomenon. It shows that the convective heat transfer is symmetric with angle-of-attack plane, whereas the surface ablation and the resulting displacement thickness are asymmetric with the incident plane. One can approximate Δ in laminar boundary-layer flow as

$$\Delta = \Delta_0 - \Delta_1 \cos(\phi - \phi_L)$$

where Δ_0 is the displacement thickness at zero angle of attack, $\Delta_1 = C_1(\alpha/\theta_C)\sqrt{(x\nu/u_e)}$ is the displacement thickness perturbation caused by missile/RV at angle of attack, and ϕ_L is the ablation lag. Here, C_1 can be expressed as a function of ablation parameters $B'$and the ablation oscillation amplitude A (e.g., $C_1 \sim B'A$). When $\phi = 0$ deg, the flow is at the windward meridian, and when $\phi = 180$ deg the flow is at the leeward plane.

The influence of heat-shield ablation on the displacement thickness in laminar flow has been correlated from numerical computations on different heat shields with chemical equilibrium and

nonequilibrium boundary-layer approximations[6–9]

$$\Delta_0/\Delta_{\dot{m}=0} = 1 + C''B' \tag{7a}$$

where

$$B' = \frac{2\dot{m}}{\rho_e u_e C_{f0}}\left(\frac{M_{\text{air}}}{M_{\text{inj}}}\right) \tag{7b}$$

$C'' = 0.33$ to 0.6 depending on the pressure gradient and wall temperature ratio.

Based on linearized aerodynamic theory, Ward[10] has derived the following simple relation for estimating the transverse force on a slender body in supersonic flow:

$$C_Y\hat{i}_y + C_N\hat{i}_z = -2\frac{\mathrm{d}\hbar}{\mathrm{d}x} \tag{8}$$

where $\hbar$ is the center of mass of the effective body including the viscous displacement effects [i.e., $r_{\text{EFFECTIVE}} = r_B + \Delta$, Eq. (5)].

After some algebraic manipulations[10,11] the yaw-force coefficient C_Y on a sharp cone can be found as

$$C_Y = C_1(\alpha/\theta_c)\sin\phi_L\,\tfrac{1}{3}\sqrt{\nu/u_e x}$$

Herein, the yaw-force coefficient is found to be proportional to the angle of attack and the ablation-lag angle ϕ_L. Because C_Y is inversely proportional to the square root of the Reynolds number and $\sqrt{(\nu/u_e x)} \ll 1$ at the altitude of interest, the magnitude of C_Y is much smaller than the normal-force coefficient, C_N, which is also proportional to angle of attack α. Similarly, the yaw-moment coefficient C_n, with its center of moment at the vertex of the cone, can be estimated as

$$C_n = C_1(\alpha/\theta_c)\sin\phi_L\,\tfrac{1}{5}\sqrt{(\nu/u_e x)}(L/L_{\text{ref}})$$

Then the center of pressure for the yaw force on a sharp cone was found to be

$$X_{\text{cp yaw}} = C_n/C_Y = 0.6$$

For an RV with c.g. location X_{cg}, the out-of-plane moment becomes

$$C_n = C_Y(X_{\text{cg}} - X_{\text{cp yaw}}) = C'\alpha$$

$$C' = C_1\frac{\sin\phi_L}{3\theta_c}\sqrt{\frac{\nu}{u_e x}}\left(\frac{X_{\text{cg}} - X_{\text{cp yaw}}}{L_{\text{ref}}}\right) \tag{9}$$

This out-of-plane moment is induced by asymmetric ablation. The parameter C_1 can be correlated with the ablation characteristics of the heat-shield materials, the amplitude A, given in Fig. 5, and the steady-state ablation rate B'. In the present investigation C_1 is approximated as

$$C_1 = 8.5B'A$$

This empirical correlation was inferred from numerical results obtained from the REACH code.[9] This correlation was developed to provide a closed-form solution, such that one can get an idea which parameters are important in the computations of the out-of-the-plane moment.

Several heat-shield materials were investigated to assess their associated ablation-lag effects during reentry flight. Table 1 lists the thermal and ablation properties of three candidate materials: carbon cloth, Teflon, and epoxy. These three materials were chosen because they represent a wide range of thermal protection materials. For instance, carbon is a high-temperature, low-ablation material. The sublimation process produces the gaseous species, whose molecular weight is similar to that of the ambient air molecules (Table 1). On the other hand, Teflon is a low-temperature ablator with a relatively high ablation rate at low altitude; its injected gaseous molecular weight is higher than the molecular weight of air. Epoxy is also a relatively high ablation rate material in a high heating environment; however, its ablated gaseous species have lower molecular weights than air. This lower molecular weight has profound influence on the magnitude of B'. Its effects can be seen from Eq. (7b). So far, no thermal ablation information is available on the BK-9 overlay material (Araldite).

The thermal parameters of all of these materials are important for the estimation of ablation lag and viscous displacement effects and the development of the asymmetric aerodynamics. The heat of ablation values Q^* and molecular weights listed in Table 1 are for laminar flow at altitudes of 80–200 kft. Using Thyson's analysis, the phase lag and oscillation amplitude for these materials can be estimated. Table 2 depicts these values at four altitudes ($h = 200$, 150, 110, and 70 kft). Above 200 kft the surface recession is negligible; therefore, the ablation lag phenomenon is not important. Below 200 kft the phase lag for carbon cloth is close to 40 deg, yet its amplitude is small ($A \approx 0.1$). The phase lag for a Teflon heat shield varies from 12 deg at 150 kft to 2 deg at 70 kft; and its amplitude A varies from 0.8 to 1.0 over the same altitude range. As for epoxy, the phase lag is 14 deg at 150 kft and 1 deg at 70 kft and the amplitude A goes from 0.9 to 1.1.

The material thermal and ablation properties would affect the viscous displacement thickness. The parameter that determines the asymmetric part of the viscous displacement thickness is $B'A\sin\phi_L$. For carbon cloth the value of $B'A\sin\phi_L$ is relatively small, about 0.04. This is not surprising because carbon has a small ablation rate in laminar flow conditions (or $B' \approx 0.175$ in the oxidation regime). For Teflon $B'A\sin\phi_L$ assumes magnitudes of 0.1–0.2 in the altitudes of interest (Table 2). On the other hand, the value of the parameter $B'A\sin\phi_L$ varies from 2.29 at 150 kft to 0.2 at 70 kft for the epoxy material. The lower molecular weight of the ablated gaseous species (as compared to nitrogen or air species) from an epoxy-coated surface [see Table 1 and Eq. (7b)] and the larger ablation rate are the major reasons that $B'A\sin\phi_L$ is higher on epoxy heat shield than that on Teflon. In turn, it results in more pronounced, asymmetric viscous displacement effects on epoxy-coated vehicle than on Teflon or carbon–carbon vehicles.

Table 1 Thermal and ablation properties of three materials

Material	Density, lb/ft^3	$\kappa \times 10^5$, BTU/ft-s-R	λ, ft^2/s	Q^*, BTU/lb	M_{inject}/M_{N2}
Carbon cloth	119	1,388	4.7×10^{-4}	~16,000	1.1
Teflon	134	2.0	9.6×10^{-7}	~5,000	1.4
Epoxy	68.8	1.5	6.3×10^{-7}	~2,500	0.38

Table 2 Ablation and lag properties of three materials

Property	Carbon				Teflon				Epoxy			
Altitude, kft	200	150	110	70	200	150	110	70	200	150	110	70
$\dot{q}$, Btu/ft^2-s	12	27	75	135	12	27	75	135	12	27	75	135
$\dot{m}$, lb/ft^{2}s	8.6^{-4}	1.93^{-3}	5.36^{-3}	9.6^{-3}	2.4^{-3}	5.4^{-3}	1.5^{-2}	2.7^{-2}	4.8^{-3}	1.08^{-2}	3.0^{-2}	5.4^{-2}
Λ	1.1^8	2.2^7	2.9^6	8.9^5	3.8^4	7.4^3	997	302	1620	321	41.7	12.9
ϕ_L, deg	45	45	45	40	45	12	5	2	45	14	5	1
A	——	0.05	0.10	0.16	——	0.81	0.95	1.0	——	0.9	1.2	1.1
$B'A\sin\phi_L$	0	0.02	0.04	0.06	0	0.24	0.12	0.05	0	2.29	1.1	0.2
$\dot{s}_0$, ft/s	0	1.62^{-5}	4.5^{-5}	8.1^{-5}	0	4.03^{-5}	1.1^{-4}	2.0^{-4}	0	1.57^{-4}	4.36^{-4}	7.85^{-4}
C'	0.0	1.46^{-5}	1.63^{-5}	9.89^{-6}	0.0	1.53^{-4}	4.19^{-5}	7.38^{-6}	0.0	1.46^{-3}	3.90^{-4}	2.99^{-5}

In all cases considered, the ablation lag becomes smaller at lower altitudes. Also the viscous displacement effects become less important at lower altitudes because of the increase in Reynolds number. Based on the present analysis, the ablation-lag and flight-dynamics divergence would become less of an issue in turbulent flow.

There are several other attributes that can also cause the advent of the out-of-plane moment. They are 1) the centrifugal force effects caused by RV spinning/precession motion coupled with the angle of attack; 2) crossflow asymmetric shear forces; 3) secondary flow separation and asymmetric vortex formation; and 4) the asymmetric transition from laminar to turbulent flows. A brief investigation into the influence of the first three attributes found them to be small compared to the viscous displacement effect.[11]

Flight Dynamics

With the out-of-plane moment just given, flight simulations can be run to assess the potential of flight-dynamics instability induced by the ablation-lag phenomena. The angle-of-attack history from the advent of this yaw moment can be found from the Platus analysis[12]

$$\alpha/\alpha_0 = \exp(-\zeta\varpi + C'\varpi^2/2\dot{\psi})t$$

where α_0 is the initial angle of attack. For illustration purposes the aerodynamic parameters ϖ, $\dot{\psi}$, and ζ are assumed to be approximately constant over the altitude of interest, such that a closed form solution can be derived as given in the preceding equation.

The angle of attack will exponentially increase when C' in the out-of-plane moment term satisfies the following condition:

$$C'(\varpi/\dot{\psi}) > 2\zeta > 0$$

Usually, the aerodynamic damping ζ is small, particularly at altitudes greater than 50 kft; therefore, a small out-of-plane moment can cause an angle-of-attack divergence. However, not all out-of-plane moments cause angle-of-attack divergence. For instance, when $C' < 0$, or $C_n < 0$ and $\dot{\psi} > 0$, there is no angle-of-attack divergence; instead, the rate of angle-of-attack convergence is faster than the case of $C_n = 0$. In another situation, when the positive precession mode ($\dot{\psi} > 0$), and an ablation lead ($\phi_L < 0$), in our notation (i.e., $C' < 0$), then $C'\varpi/\dot{\psi} < 0$. In this case the out-of-plane moment also causes a more rapid convergence of the angle of attack. Similarly, for the negative precession mode $\dot{\psi} < 0$, with ablation phase lag ($\phi_L > 0$), the result is $C'\varpi/\dot{\psi} < 0$. Consequently, ablation lag with a negative precession mode also causes a faster angle-of-attack convergence.

Chrusciel[13] found, in his analysis of reentry vehicles with relatively large initial angles of attack at high altitude, that the RV motion generally converges at a negative precession rate. The asymmetric outgassing (ablation) on a charring ablator gives a positive moment for an ablation lag, resulting in a more rapid convergence of the angle of attack (because $\dot{\psi} < 0$, $\phi_L > 0$, and $C'\varpi/\dot{\psi} < 0$). However, in most cases of reentry dynamics the initial precession rate is positive for small initial angles of attack; and for $(X_{cg} - X_{cp\,yaw}) > 0$, the ablation lag results in angle-of-attack divergence.

Six-degree-of-freedom simulations were made with the out-of-plane moment given in Eq. (9) and in Table 2 (and Fig. 8) for the three heat-shield materials. Figure 9 depicts the numerical results for the angle-of-attack history for epoxy. Angle-of-attack divergence is seen at about 145 kft altitude, and it starts to converge below 90 kft. The corresponding ballistic coefficient history during reentry flight is shown in Fig. 10. A drop in the ballistic coefficient between the altitude $145 > h > 85$ kft is attributed to the increase in the drag coefficient caused by the angle-of-attack divergence. In the cases of carbon and Teflon, no angle-of-attack divergence was found in the six-degree-of-freedom simulations (Fig. 9). This is because the yaw moment C_n for Teflon is an order of magnitude smaller than that for epoxy, and C_n is almost two orders of magnitude less for carbon cloth as compared to epoxy.

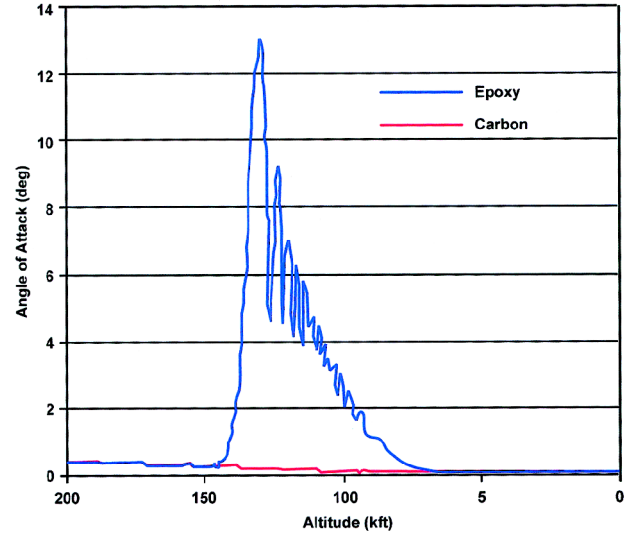

Fig. 9 Angle-of-attack history for a slender cone with epoxy and carbon heat shields.

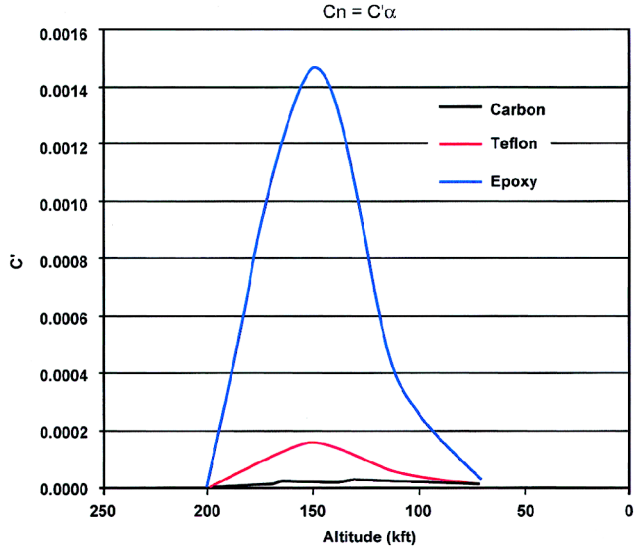

Fig. 8 Predicted out-of-plane moment history on a slender cone for epoxy, Teflon, and carbon heat shields.

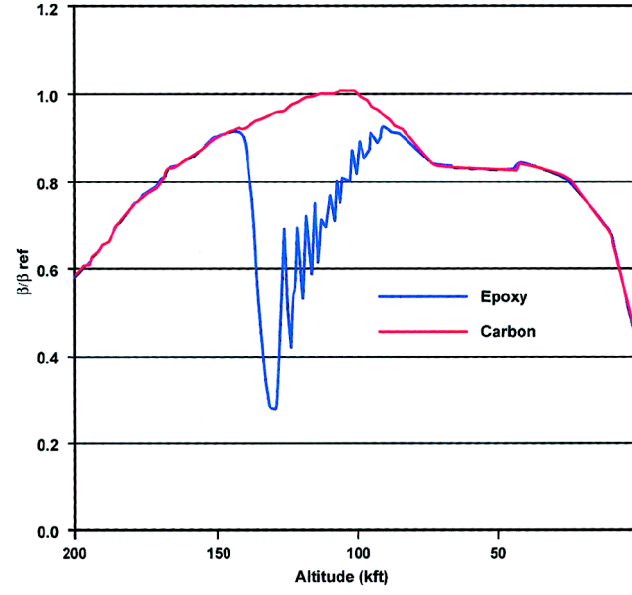

Fig. 10 Ballistic coefficient history for a slender cone with epoxy and carbon heat shields.

In summary, our analytical model indicated that at high altitude ($h > 150$ kft) the ablation rate $\dot{m}$ is small so that $\Lambda \gg 1$ and the phase lag approaches 45 deg, but the asymmetric ablation amplitude is small ($A \to 0$). Consequently, the out-of-plane moment induced by the viscous displacement effect is small, and it would not cause angle-of-attack divergence. At lower altitude ($h < 80$ kft) the ablation rate becomes large so that $\Lambda \leq 1$, and the phase lag assumes small values ($\phi_L \to 0$ deg). Therefore, the out-of-plane moment becomes small again, and no flight dynamic instability would occur. Some researchers refer to this low altitude angle-of-attack convergence as a "healing" effect. Only at an intermediate altitude, where the ablation phase lag ϕ_L and amplitude A are finite, are flight instability and angle-of-attack divergence likely to occur. But the effects of the precession motion, the RV center of mass location, and the heat-shield material ablation characteristics are also important factors that determine the possible advent of flight instability as observed on Black Knight-9.

Summary

An analytical model is proposed to assess the ablation-lag phenomena. The magnitude of ablation phase lag, and its oscillation magnitude for noncharring materials was estimated from the one-dimensional transient heat-conduction equation. Based on this ablation-lag result (Fig. 5), an aerodynamic model was developed to estimate the Magnus moment (or out-of-plane moment). The Magnus moment is produced by the combined effects of heat-shield ablation mass addition, reentry vehicle spin, and angle of attack. The magnitude of the Magnus moment not only depends on the phase lag ϕ_L, but also on amplitude A. Consequently, it depends on the thermal properties of the heat-shield material, the local Reynolds number, and the RV spin rate and center of gravity position.

Important heat-shield thermal properties include the heat of ablation, thermal diffusivity, and the molecular weight of the ablated gas. Therefore, the heat-shield material plays a major role in determining the high-altitude performance of a reentry vehicle. In other words, heat shields with certain thermal and ablative properties would be vulnerable to flight-dynamics instability.

References

[1]Waterfall, A. P., "Effect of Ablation on the Dynamics of Spinning Re-Entry Vehicles," *Journal of Spacecraft and Rockets*, Vol. 6, No. 9, 1969, pp. 1038–1044.

[2]Morrison, A. M., and Fiscina, C., "Effects of Spin and Mass Addition on High-Angle-of-Attack-Re-Entry," *Journal of Spacecraft and Rockets*, Vol. 22, No. 1, 1985, pp. 68–73.

[3]Martellucci, A., and Neff, R. S., "The Influence of Asymmetric Transition on Re-Entry Vehicle," AIAA Paper 70-987, Aug. 1970.

[4]Thyson, N. A., "The Ablation Response of Oscillating Bodies," Avco System Div., BSD-TR-66-237, Wilmington, MA, Aug. 1966.

[5]Thyson, N. A., "A Linearized Analysis Concerning Boundary Layer Effects on the Static and Dynamic Behavior of Slender, Ablating and Non-Ablating Bodies," Avco, RAD TM-64-34, Wilmington, MA, June 1964.

[6]Nestler, D. E., "Approximate Calculation of Laminar Boundary Layer Development, Including Mass Addition," General Electric Missile and Space Div., Philadelphia, May 1969.

[7]Lagnanelli, A. L., Fogaroli, R. P., and Martellucci, A., "The Effects of Mass Transfer and Angle of Attack on Hypersonic Turbulent Boundary Layer Characteristics," U.S. Air Force Flight Dynamics Lab., AFFDL-TR-75-35, Philadelphia, April 1975.

[8]Kendall, R. M., "A Multicomponent Boundary Layer Chemically Coupled to an Ablating Surface," *AIAA Journal*, Vol. 5, No. 6, 1967, p. 1063.

[9]Hall, D. W., "Reentry Aerothermal Chemistry," AFSC, BMO-TR-94-29, Valley Forge, PA, April 1994.

[10]Ward, G. N., "Supersonic Flow Past Slender Pointed Bodies," *Quarterly Mechanics and Applied Mathematics*, Vol. 2, No. 1, 1949, p. 75.

[11]Lin, T. C., and Rubin, S. G., "Viscous Flow over Spinning Cones at Angle of Attack," *AIAA Journal*, Vol. 12, No. 7, 1974, pp. 975–985.

[12]Platus, D. H., "Ballistic Re-Entry Vehicle Flight Dynamics," *Journal of Guidance and Control*, Vol. 5, No. 1, 1982, p. 4.

[13]Chrusciel, G., "Analysis of Asymmetric Mass Addition Effects on Hypersonic Flow Field Characteristics," AIAA Paper 99-0433, Jan. 1999.

W. E. Williamson
Associate Editor

Color reproductions courtesy of Northrop Grumman Mission Systems.